

Supplementary Information

Facile synthesis of “digestible”, rigid-and-flexible, and bio-based building block for high-performance degradable thermosetting plastics

Binbo Wang^{1,2}, Songqi Ma^{1*}, Qiong Li^{1,4}, Hua Zhang¹, Junjie Liu³, Rong Wang¹, Zhiquan Chen³, Xiwei Xu¹, Sheng Wang^{1,4}, Na Lu^{1,4}, Yanlin Liu¹, Shifeng Yan², Jin Zhu¹

¹ Key Laboratory of Bio-based Polymeric Materials Technology and Application of Zhejiang Province, Division of Polymers and Composites, Ningbo Institute of Materials Technology and Engineering, Chinese Academy of Sciences, Ningbo 315201, P. R. China;

² School of Materials Science and Engineering, Shanghai University, Shanghai 200072, P. R. China;

³ School of Physics and Technology, Wuhan University, Wuhan 430000, P. R. China;

⁴ University of Chinese Academy of Sciences, Beijing 100049, P. R. China.

*Corresponding authors: (Songqi Ma) E-mail: masongqi@nimte.ac.cn, Tel: 86-574-87619806

Contents

Supplementary Figures	3
Fig. S1 DSC curves of HMDO and DGHMDO.	3
Fig. S2 Hydrolysis of HMDO in 0.1 M hydrochloric acid solution (DMSO-d ⁶ /H ₂ O=9/1, v/v), ^a the ratio is the percentage of HMDO in the undegraded acetals.	4
Fig. S3 Hydrolysis of HMDO in 0.01M hydrochloric acid solution (DMSO-d ⁶ /H ₂ O=9/1, v/v), ^a the ratio is the percentage of HMDO in the undegraded acetals.	5
Fig. S4 Real-time ¹ H NMR spectra of HMDO degradation in 0.001M HCl solution (DMSO-d ⁶ /H ₂ O=9/1, v/v) at 23 °C.	6
Fig. S5 Real-time ¹ H NMR spectra of HMDO degradation in 0.01M HCl solution (DMSO-d ⁶ /H ₂ O=9/1, v/v) at 23 °C.	7
Fig. S6 Real-time ¹ H NMR spectra of HMDO degradation in 0.1M HCl solution (DMSO-d ⁶ /H ₂ O=9/1, v/v) at 23 °C.	8
Fig. S7 Non-isothermal DSC curves of DGHMDO and DDM mixtures at different heating rates (5 °C min ⁻¹ , 10 °C min ⁻¹ , 15 °C min ⁻¹ and 20 °C min ⁻¹).	9
Fig. S8 ln (q/T_p^2) as a function of $1/T_p$ based on Kissinger's theory.	10
Fig. S9 ln q as a function of $1/T_p$ based on Ozawa's method.	11
Fig. S10 Contact angle of different solvents on DGHMDO-DDM.	12
Fig. S11 Appearance of DGHMDO-DDM before and after immersing in 0.1 M NaOH aqueous solution, water, 0.1 M HCl aqueous solution at 25 °C and 50 °C for 48 h.	13
Fig. S12 TGA curves of HMDO and DGHMDO.	14
Supplementary Tables	15
Table S1 Selected Bond Lengths (Å) in HMDO and BPA	15
Table S2 Coating performance of the thermosetting plastics	16
Table S3 Analyzed data for the positron lifetime of the thermosetting plastics.....	17
Table S4 Degradation ratio of DGHMDO-DDM under different conditions	18
Table S5 Chemical stability of DGHMDO-DDM in deionized water, hydrochloric acid aqueous solution and sodium hydroxide aqueous solution.....	19
Supplementary Methods	20

Supplementary Figures

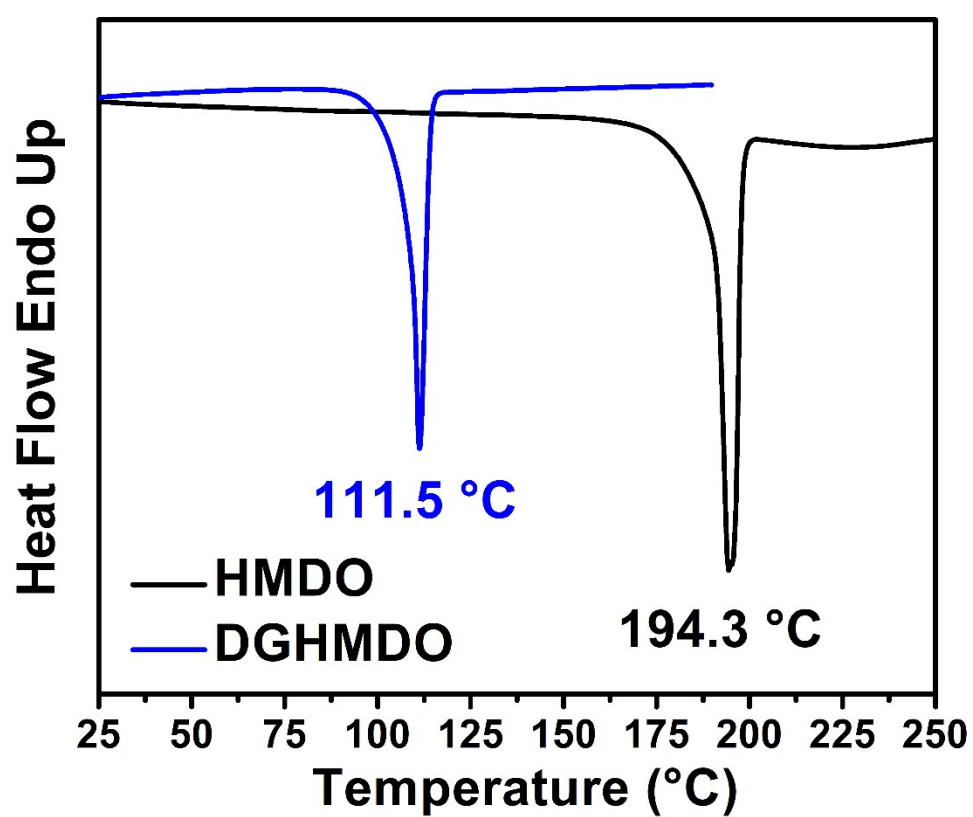


Fig. S1 DSC curves of HMDO and DGHMDO.

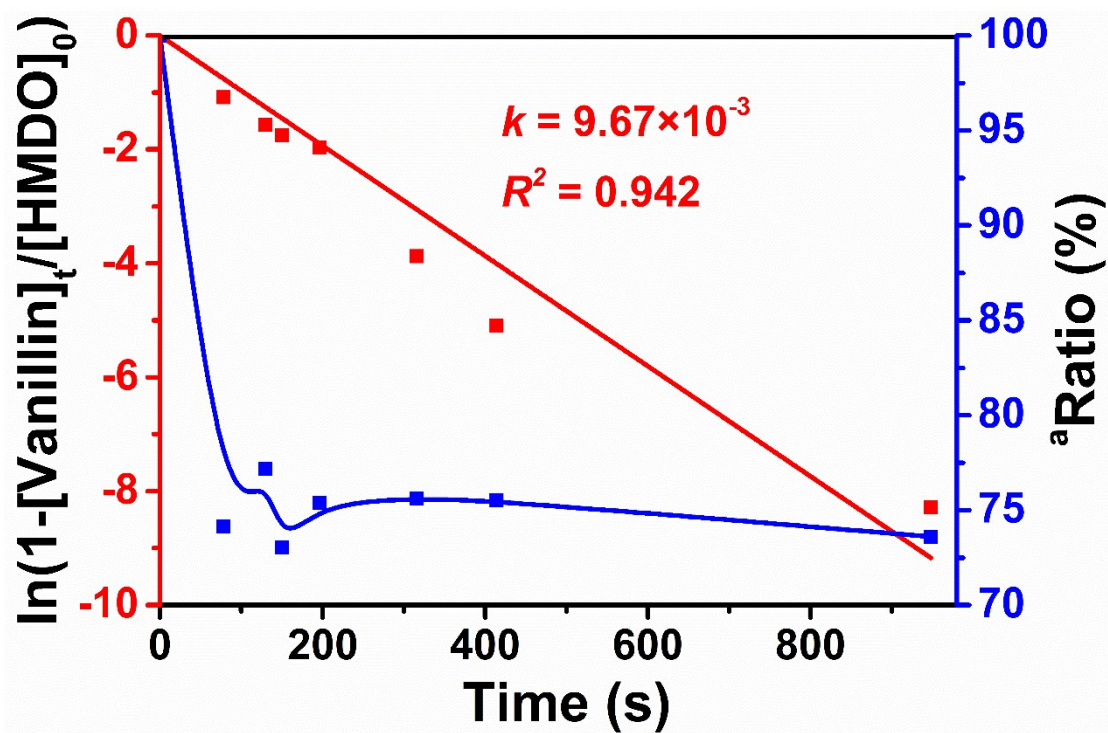


Fig. S2 Hydrolysis of HMDO in 0.1 M hydrochloric acid solution (DMSO-d⁶/H₂O=9/1, v/v), ^a the ratio is the percentage of HMDO in the undegraded acetals.

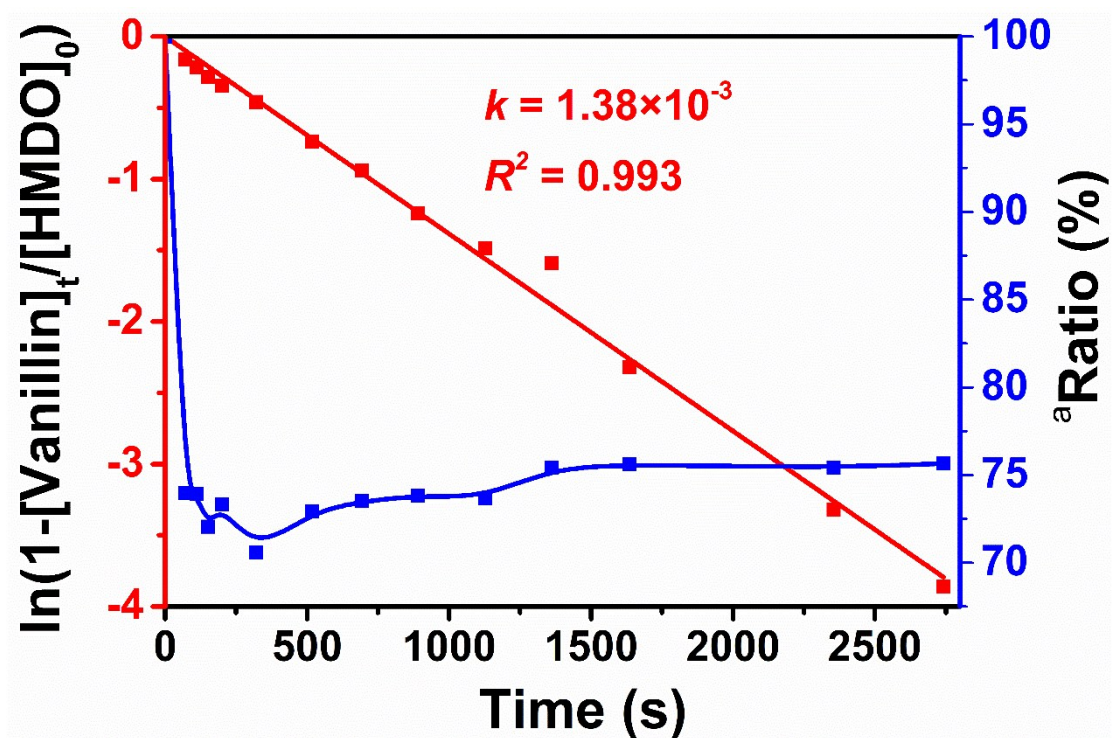


Fig. S3 Hydrolysis of HMDO in 0.01M hydrochloric acid solution (DMSO-d⁶/H₂O=9/1, v/v), ^athe ratio is the percentage of HMDO in the undegraded acetals.

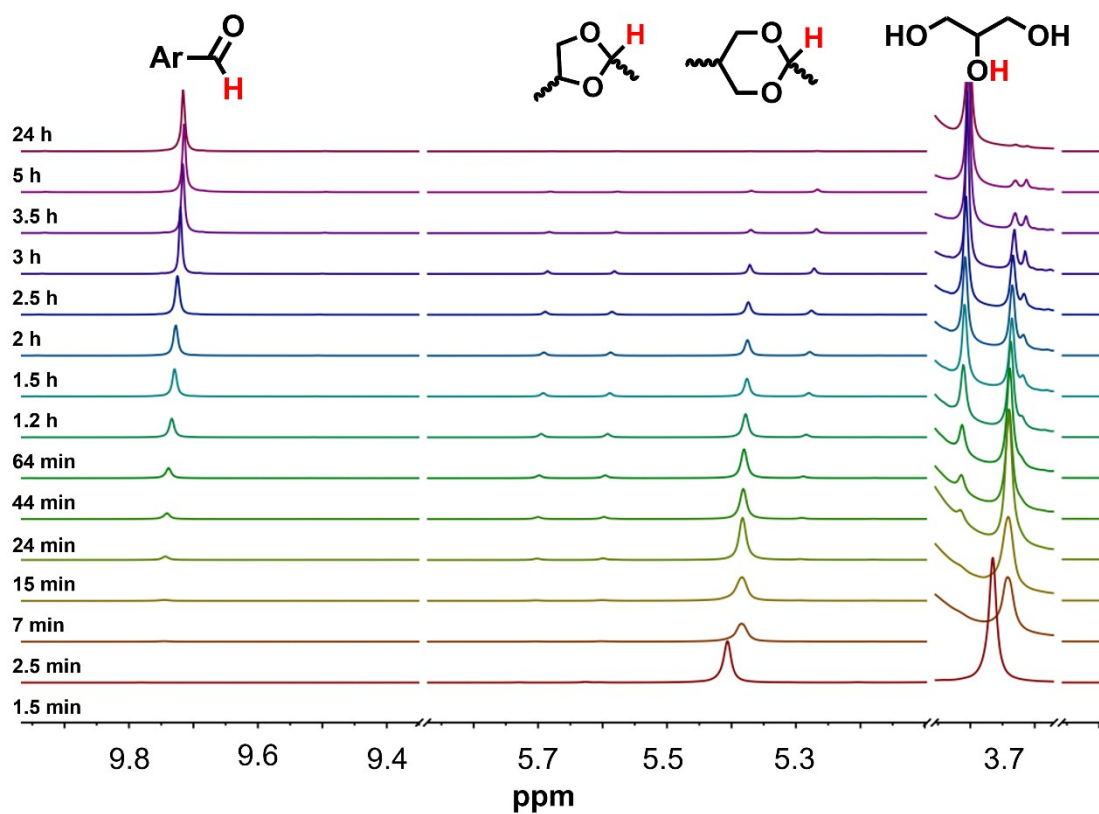


Fig. S4 Real-time ¹H NMR spectra of HMDO degradation in 0.001M HCl solution (DMSO-d⁶/H₂O=9/1, v/v) at 23 °C.

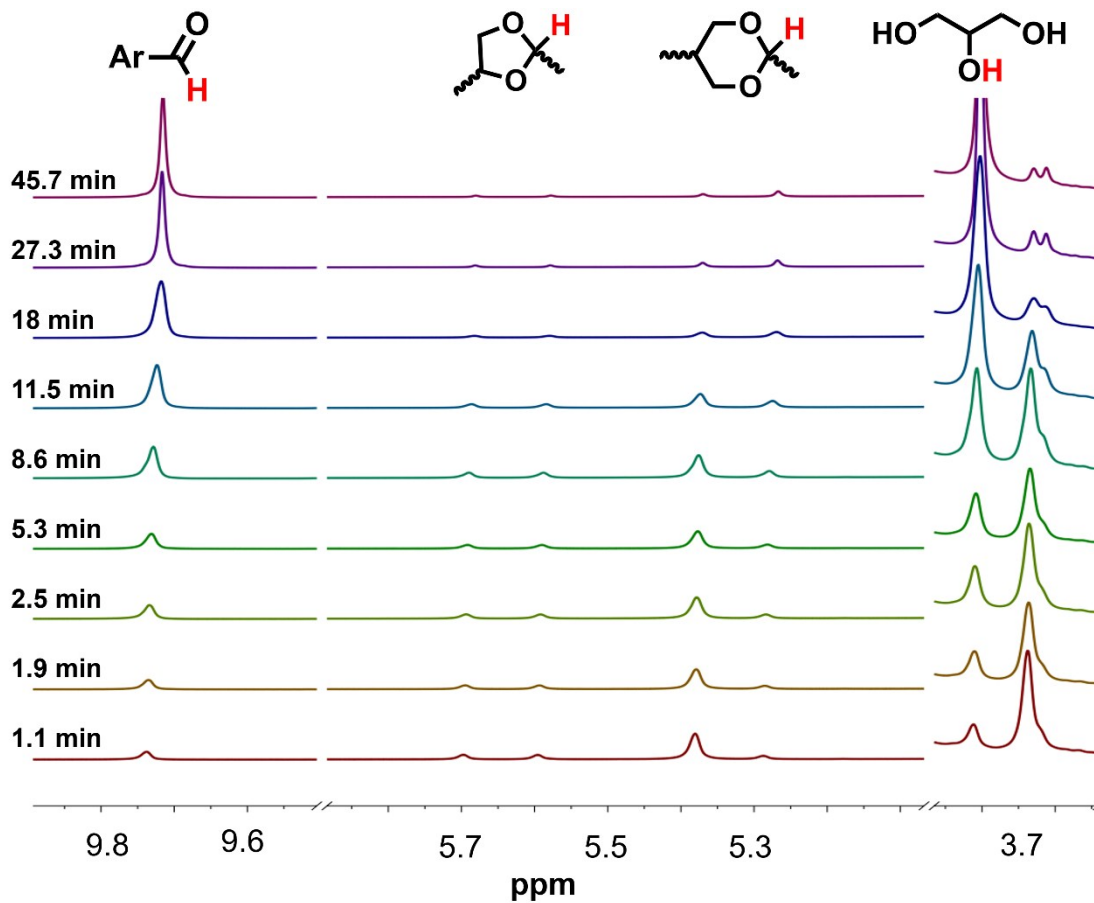


Fig. S5 Real-time ^1H NMR spectra of HMDO degradation in 0.01M HCl solution (DMSO- d_6 /H $_2$ O=9/1, v/v) at 23 °C.

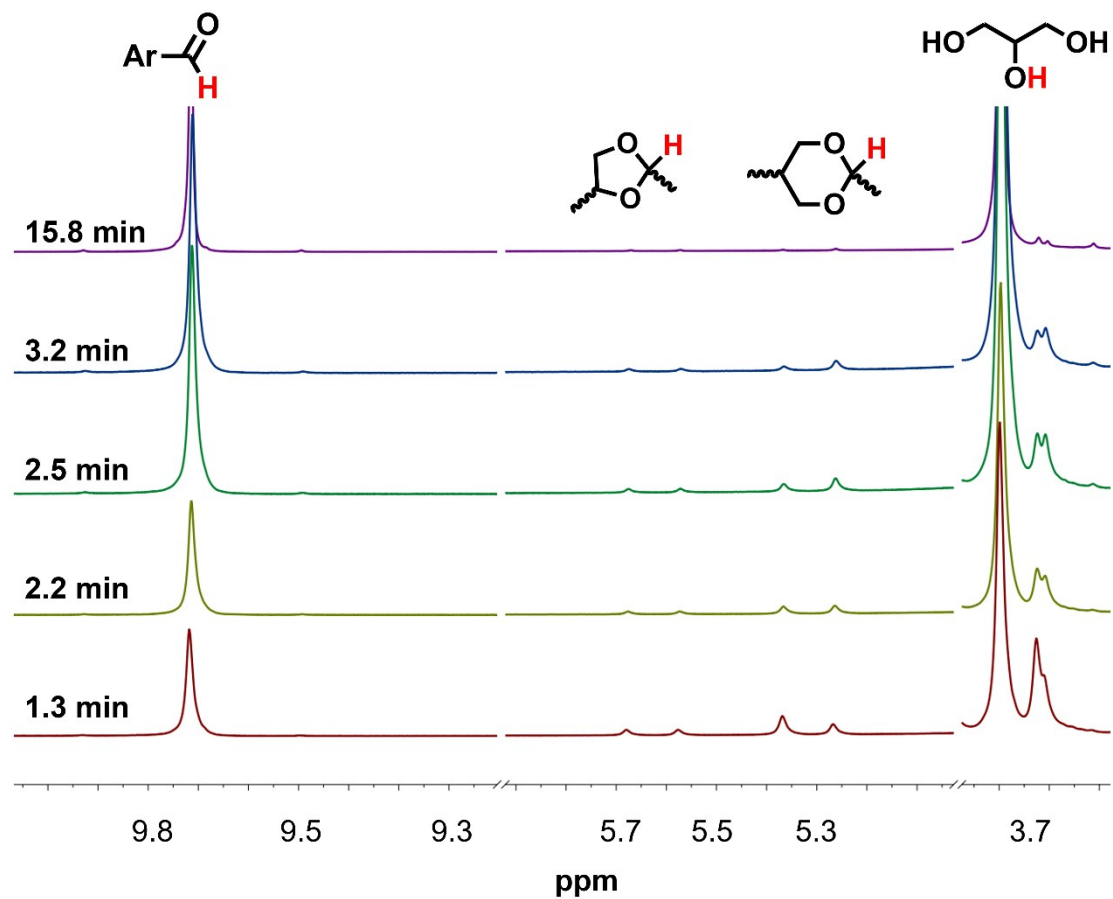


Fig. S6 Real-time ^1H NMR spectra of HMDO degradation in 0.1M HCl solution (DMSO- d_6 /H $_2$ O=9/1, v/v) at 23 °C.

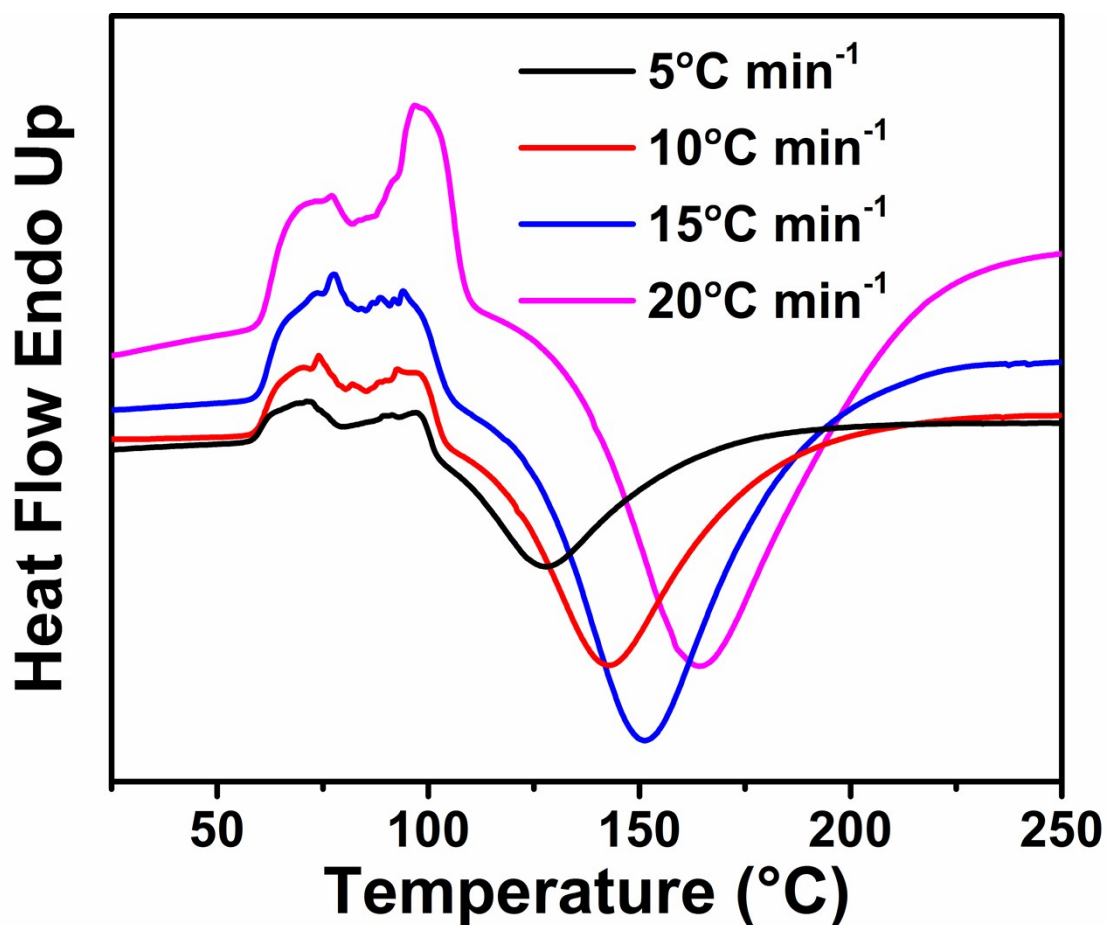


Fig. S7 Non-isothermal DSC curves of DGHMDO and DDM mixtures at different heating rates (5 °C min⁻¹, 10 °C min⁻¹, 15 °C min⁻¹ and 20 °C min⁻¹).

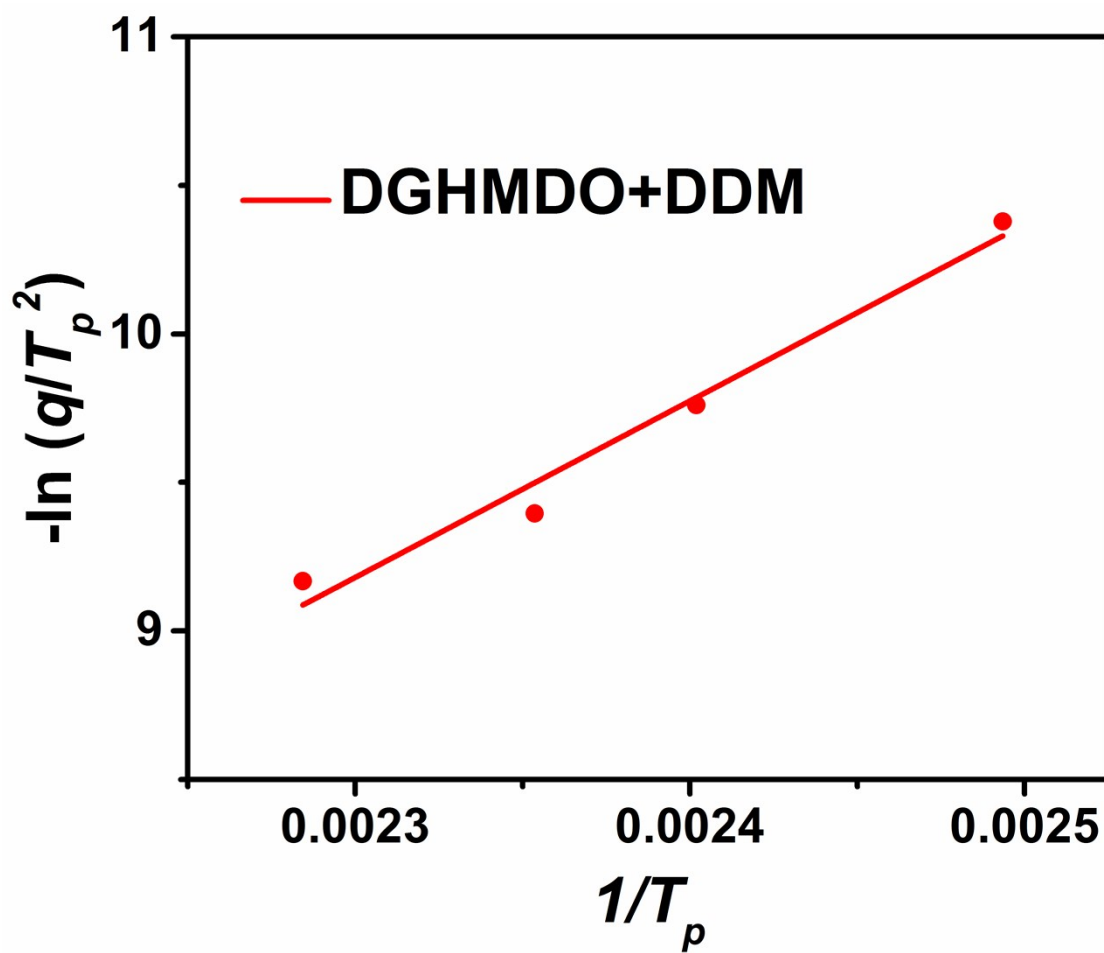


Fig. S8 $\ln(q/T_p^2)$ as a function of $1/T_p$ based on Kissinger's theory.

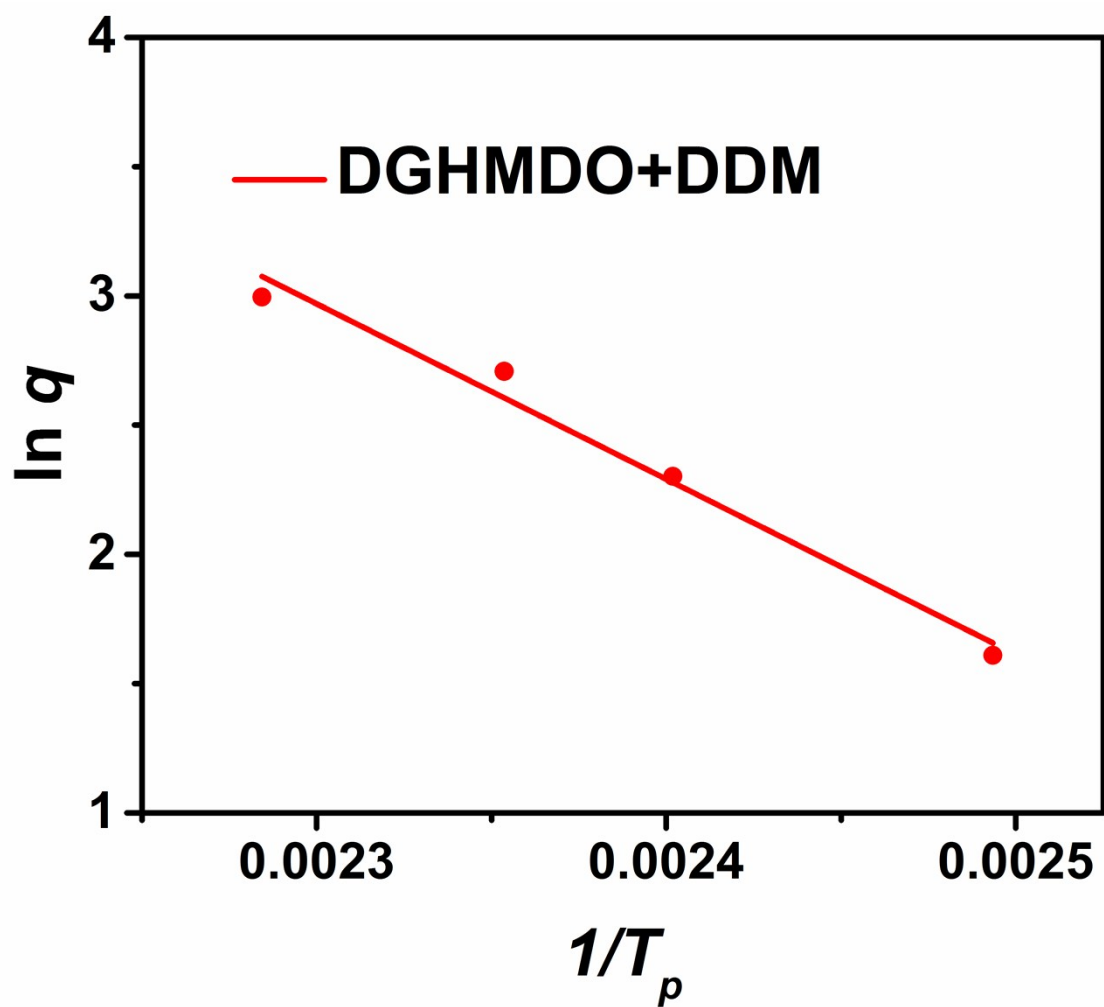


Fig. S9 $\ln q$ as a function of $1/T_p$ based on Ozawa's method.

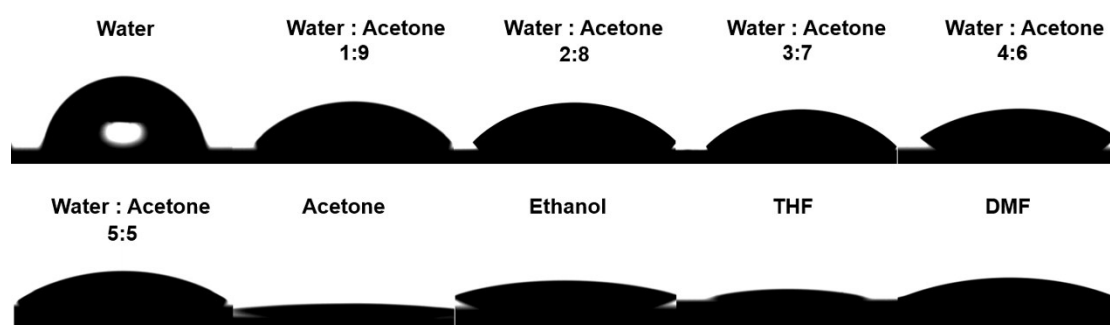


Fig. S10 Contact angle of different solvents on DGHMDO-DDM.

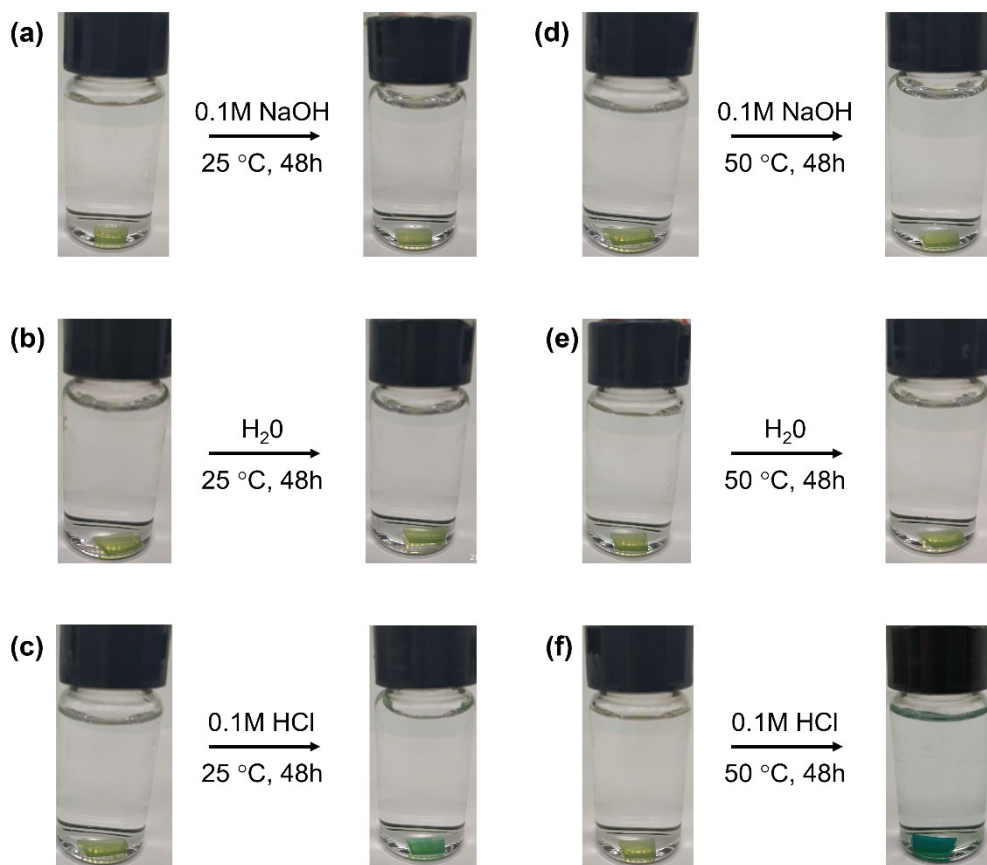


Fig. S11 Appearance of DGHMDO-DDM before and after immersing in 0.1 M NaOH aqueous solution, water, 0.1 M HCl aqueous solution at 25 °C and 50 °C for 48 h.

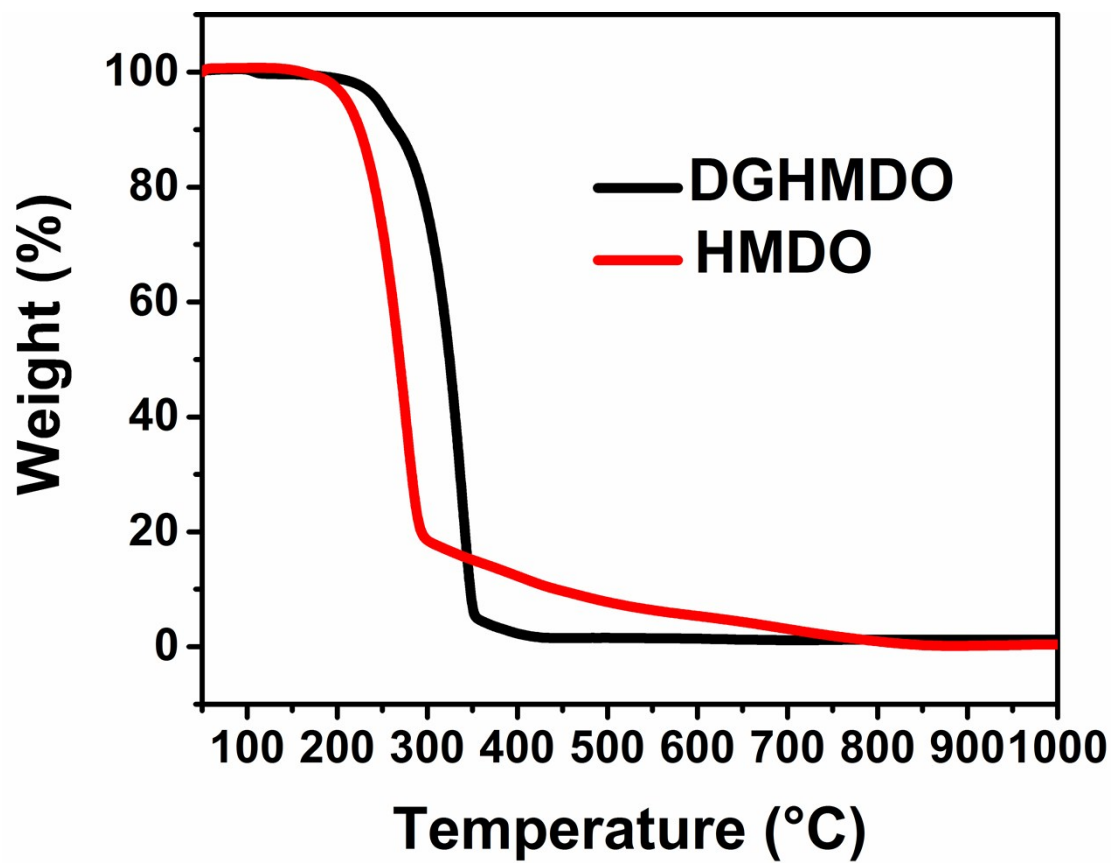


Fig. S12 TGA curves of HMDO and DGHMDO.

Supplementary Tables

Table S1 Selected Bond Lengths (Å) in HMDO and BPA

HMDO		BPA	
C(1)-O(2)	1.41326	C(1)-C(4)	1.3883
O(2)-C(3)	1.36895	C(4)-C(5)	1.39854
C(3)-C(8)	1.4015	C(5)-C(6)	1.38029
C(3)-C(4)	1.38023	C(6)-C(7)	1.39159
C(4)-C(5)	1.39574	C(7)-C(9)	1.38508
C(5)-C(6)	1.384	C(9)-C(1)	1.39161
C(6)-C(7)	1.3907	C(7)-O(8)	1.36157
C(7)-C(8)	1.38009	C(4)-C(3)	1.53433
C(8)-O(9)	1.3548	C(2)-C(3)	1.53859
C(5)-C(10)	1.50377	O(8)-H	0.96084
C(10)-O(11)	1.40625		
O(11)-C(12)	1.41658		
C(12)-C(13)	1.52029		
C(13)-O(14)	1.41391		
O(9)-H	0.96518		
O(14)-H	0.95993		

Table S2 Coating performance of the thermosetting plastics

Sample	DGHMDO-DDM	DGEBA-DDM
Pencil hardness	5H	6H
Crosshatch adhesion	3B	2B
Reverse impact strength	45 cm.-kg	35 cm.-kg

Table S3 Analyzed data for the positron lifetime of the thermosetting plastics

Sample	τ_3 (ns)	I_3 (%)	r_{PLAS}^a (Å)	V_{PLAS}^b (Å ³)	f_V^c (%)
DGHMDO-DDM	1.55	26.04	2.394	57.47	2.69
DGEBA-DDM	1.77	29.80	2.628	76.03	4.08

Table S4 Degradation ratio of DGHMDO-DDM under different conditions

Adjusted condition	Main solvent	Acid	Concentration (M)	Temperature (°C)	Volume ratio (water/main solvent)	Time (h)	Degradation ratio (%)
Temperature	Acetone	HCl	0.1	25	1/9	12	5.46
	Acetone	HCl	0.1	50	1/9	5.5	100
The type of main solvent	THF	HCl	0.1	50	1/9	6	100
	Acetone	HCl	0.1	50	1/9	5.5	100
	Ethanol	HCl	0.1	50	1/9	12	57.17
	Methanol	HCl	0.1	50	1/9	12	56.48
	DMF	HCl	0.1	50	1/9	12	3.92
	DMSO	HCl	0.1	50	1/9	12	-0.7
The type of acid	Acetone	HCl	0.1	50	1/9	5.5	100
	Acetone	H ₂ SO ₄	0.1	50	1/9	12	42.65
	Acetone	H ₃ PO ₄	0.1	50	1/9	12	93.34
	Acetone	Acetic acid	0.1	50	1/9	12	-0.24
The concentration of acid	Acetone	HCl	1	50	1/9	0.5	100
	Acetone	HCl	0.5	50	1/9	1	100
	Acetone	HCl	0.1	50	1/9	5.5	100
The ratio of water/main solvent	Acetone	HCl	0.1	50	0.5/9.5	1.5	100
	Acetone	HCl	0.1	50	1/9	5.5	100
	Acetone	HCl	0.1	50	2/8	12	84.33
	Acetone	HCl	0.1	50	3/7	12	69.39
	Acetone	HCl	0.1	50	4/6	12	68.61
	Acetone	HCl	0.1	50	5/5	12	69.02
	No	HCl	0.1	50	10/0	12	3.13

Table S5 Chemical stability of DGHMDO-DDM in deionized water, hydrochloric acid aqueous solution and sodium hydroxide aqueous solution

Solvent	Concentration (M)	Temperature (°C)	Time (h)	Degradation ratio (%)
Deionized water	-	25	48	0
Hydrochloric acid aqueous solution	0.1	25	48	6.4
Sodium hydroxide aqueous solution	0.1	25	48	0
Deionized water	-	50	48	0
Hydrochloric acid aqueous solution	0.1	50	48	32.1
Sodium hydroxide aqueous solution	0.1	50	48	0

Supplementary Methods

Thermal stability:

The thermal stability of polymers is often indicated by the statistic heat-resistant index (T_s) which is calculated through (equation 1) with $T_{d5\%}$ (degradation temperature of 5% weight loss) and $T_{d30\%}$ (degradation temperature of 30% weight loss).²

$$T_s = 0.49 [T_{d5\%} + 0.6 (T_{d30\%} - T_{d5\%})] \quad (1)$$

Curing kinetics of DGHMDO and DDM:

The activation energy of the epoxy systems was determined by Kissinger's method (equation 2) and Ozawa's method (equation 3).³

$$- \ln (q/T_p^2) = E_a/RT_p - \ln (AR/E_a) \quad (2)$$

$$\ln q = -1.052 \times E_a/RT_p + \ln(AE_a/R) - \ln F(x) - 5.331 \quad (3)$$

Where q is the heating rate, T_p is the peak exothermic temperature, E_a is an average activation energy of the curing reaction, A is the pre-exponential factor, R is the gas constant, and $F(X)$ is a conversion dependent term. Table S3 summarizes the T_p and its corresponding heating rate.

The E_a s were calculated from the slope of the plots of $-\ln (q/T_p^2)$ versus $1/T_p$ based on Kissinger's theory or $\ln (q)$ versus $1/T_p$ based on Ozawa's method, which are presented in Figure S15-S16.

The cross-link density of the thermosetting plastics was estimated by the average molecular weight between cross-link points (M_c) which was reckoned in terms of equation 4.

$$M_c = \frac{n_{epoxy} \cdot M_{epoxy} + n_{DDM} \cdot M_{DDM}}{n_{DDM}} \quad (4)$$

where n is the amount of the corresponding component of the epoxy resin and M is the molecular weight of the corresponding component of the epoxy resin. The calculation results are summarized in the Table S6.

Calculation of the free volume (f_v) of the thermosetting plastics:

The long-lifetime component τ_3 is attributed to "pick-off" annihilation of o-Ps at holes in the amorphous phase and can be used to estimate the size of the free volumes in the amorphous

phases by equation 5.⁴

$$\tau_{0-Ps}^{-1} = 2 \left[1 - \frac{R}{R + \Delta R} + \frac{1}{2\pi} \sin\left(\frac{2\pi R}{R + \Delta R}\right) \right] \quad (5)$$

Where R is the radius of free volume hole and $\Delta R = 0.1656$ nm is derived from fitting the observed o-Ps lifetimes in molecular solids with known hole sizes. The formation probability of o-Ps, I_3 , is correlated with the intensity of the free volume.

The free volume radius R is calculated by the formula (6), and the free volume size is calculated by equation 6.

$$V = 4\pi R^3/3 \quad (6)$$

The volume fraction of the free volume, which is the percentage of the total volume of the polymer, expressed in f_v , can be calculated using equation (7), where C is a constant 0.0018 \AA^{-3} .

$$f_v = C \times I_3 \times V_f \quad (7)$$

References

- 1 S. Wang, S. Ma, C. Xu, Y. Liu, J. Dai, Z. Wang, X. Liu, J. Chen, X. Shen, J. Wei and J. Zhu, *Macromolecules*, 2017, 50, 1892-1901.
- 2 H. H. Horowitz and G. Metzger, *Anal. Chem.*, 1963, 35, 1464-&.
- 3 D. Guan, Z. Cai, X. Zhai, W. Yao, S. Wang, H. An and X. Qiu, in *Advances in Materials and Materials Processing*, Pts 1-3, eds. Z. Y. Jiang, X. H. Liu, S. H. Jiao and J. T. Han, 2013, vol. 652-654, pp. 121-+.
- 4 S. Tao, *J. Chem. Phys.*, 1972, 56, 5499-5510.